

# Suspended Carbon Nanotube Quantum Wires with Two Gates

Jien Cao, Qian Wang, Dunwei Wang, and Hongjie Dai\*

**S**uspended single-walled carbon nanotube devices comprised of high-quality electrical contacts and two electrostatic gates per device have been prepared. Compared to nanotubes pinned on substrates, the suspended devices exhibit little hysteresis related to environmental factors and act as cleaner Fabry–Perot interferometers or single-electron transistors. The high-field saturation currents in the suspended nanotubes related to optical phonon or zone-boundary phonon scattering are significantly lower due to the lack of efficient heat sinking. The multiple-gate design may also facilitate future investigations into the electromechanical properties of nanotube quantum systems.

## Keywords:

- carbon nanotubes
- chemical vapor deposition
- electron transport
- quantum dots

In recent years, successful fabrication of suspended single-walled carbon nanotube (SWNT) devices with electrical wiring has facilitated the investigation of the electrical, mechanical, and electromechanical properties of these novel wires.<sup>[1–6]</sup> Here, we report a reliable method for the fabrication of suspended SWNT devices with improved metal–nanotube contacts and a useful double-gate design. These devices have led to the discovery of some interesting electrical transport properties of nanotubes that are distinct from those pinned on substrates.

The structure of our suspended SWNT device is shown in Figure 1. It consists of a nanotube suspended over a trench by two preformed source (S) and drain (D) metal electrodes, a metal local gate ( $V_{GL}$ ) at the bottom of the trench and a global Si back gate ( $V_{GB}$ ). Device fabrication started with deposition of a 38 nm-thick  $\text{Si}_3\text{N}_4$  film on a p-type  $\text{SiO}_2/\text{Si}$  wafer ( $\text{SiO}_2$  thickness = 500 nm). Electron-beam lithography (EBL) was used to define the local-gate pattern, dry-etching and wet-etching were used to open a window in the EBL resist and  $\text{Si}_3\text{N}_4$  film and to further etch  $\approx 300$  nm deep into the  $\text{SiO}_2$  to form a trench with undercut (Figure 1a). Electron-beam deposition of Pt/W (25 nm Pt; 5 nm W as sticking layer) followed by lift-off was then carried out to complete the formation of the trench with a Pt/W local-gate electrode at the bottom. A second-step EBL

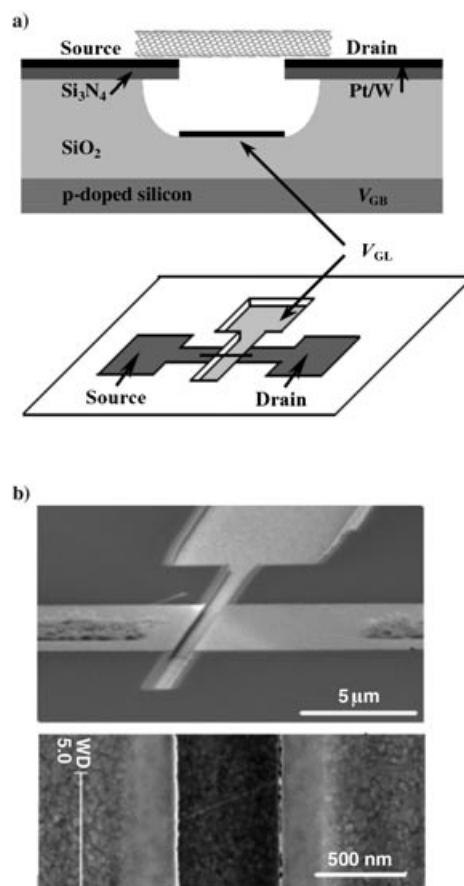


**Figure 1.** a) A schematic representation of the device structure; b) SEM images of a device consisting of a single suspended SWNT and two gates (local gate  $V_{GL}$  and global back gate  $V_{GB}$ ).

[\*] J. Cao, Dr. Q. Wang, D. Wang, Prof. H. Dai  
Department of Chemistry and Laboratory for Advanced Materials  
Stanford University, Stanford, CA 94305 (USA)  
Fax: (+1) 650-725-0259  
E-mail: hdai@stanford.edu

was performed to define the S/D pattern, followed by deposition of 5 nm W (as the sticking layer) and 25 nm Pt, and then lift-off. The region across the trench was written into a continuous stripe in the second EBL step. After metal deposition and lift-off, the stripe gave rise to the S and D electrodes separated by the trench. The S and D electrodes extended to the two edges of the trench and were electrically isolated from the local Pt gate due to undercutting in the sidewall of the trench. Finally, a third EBL step was carried out to pattern catalyst islands on top of the S and D electrodes. Chemical vapor deposition (CVD) was then used to grow SWNTs to bridge the electrode pairs on the wafer chip.<sup>[4,5]</sup> Low-yield growth conditions were used (800–825 °C) to afford mostly single tubes bridging the S/D pairs, as confirmed by scanning electron microscopy (SEM) after electrical measurements of the devices. The results presented here were all obtained from individual suspended SWNT devices.

Earlier, we described the CVD growth of SWNTs across preformed Mo electrodes for electrical and electromechanical devices.<sup>[4]</sup> Mo was chosen as the S and D electrode material due to its compatibility with SWNT growth and for its ability to be dry-etched for electrode patterning. In the current work, our fabrication process does not involve dry-etching of metal and thus allows a wider choice of refractory metals. We succeeded in using refractory metals W and Pt/W (W as adhesive layer for Pt) as preformed electrodes and found that the typical resistance of our individual suspended SWNT devices was in the range of 10–50 k $\Omega$  (Figures 2 to 4). The contact resistance appeared higher than devices with nanotubes lying on substrates with Pd top-contacts,<sup>[7,14]</sup> but lower compared to other suspended SWNT devices including those with preformed Mo electrodes.<sup>[4]</sup>

We observed several interesting properties for suspended SWNTs that are distinct from nanotubes pinned on substrates. The first is that the suspended SWNT devices are “hysteresis-free” for all samples that we have measured (more than 100 devices): they show a small amount of hysteresis in current versus gate ( $I_{sd}$  versus  $V_{GL}$ ) sweeps measured immediately after CVD growth, but the hysteresis complete-



#### Editorial Advisory Board Member

Hongjie Dai is an Associate Professor in the Chemistry Department and Laboratory of Advanced Materials at Stanford University. He received his BA in Applied Physics from Tsinghua University (P. R. China), and his PhD in Physical Chemistry from Harvard University. He has been at Stanford since 1997 following post-doctoral research at Rice University. His research program interfaces the chemistry, physics, and biological applications of novel nanostructured materials including carbon nanotubes and nanowires. He has developed methods to obtain various carbon nanotube structures on surfaces, carried out fundamental electrical, mechanical, and electromechanical studies of nanomaterials, and investigated their application in molecular electronics and as sensors. His awards include the American Chemical Society Pure Chemistry Award and a Packard Fellowship for Science and Engineering.

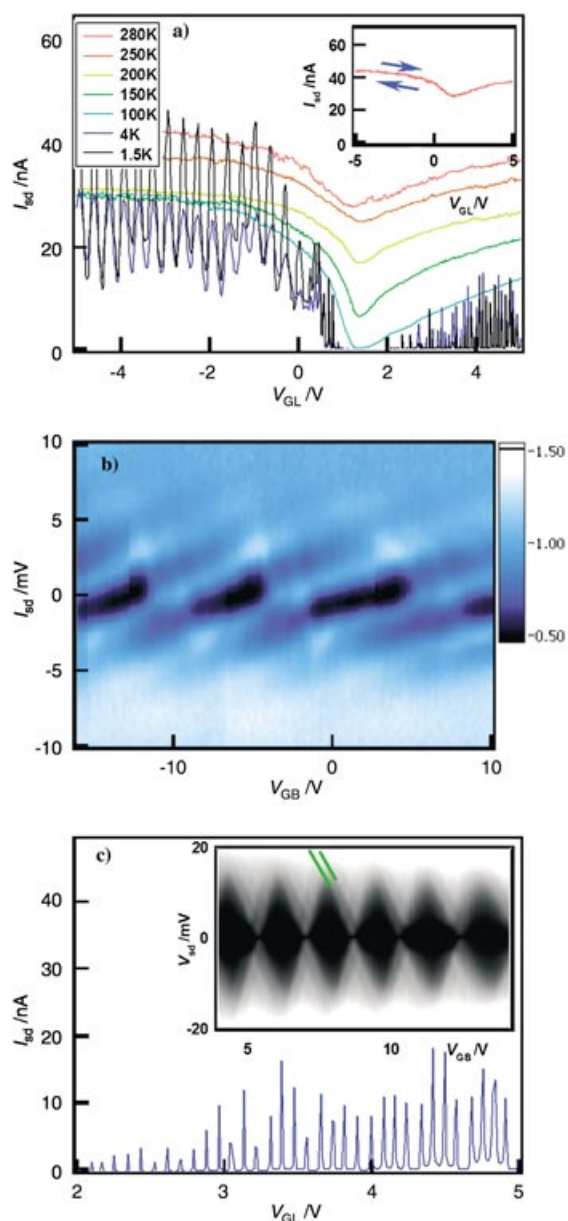


**Figure 2.** a)  $I_{sd}$  versus  $V_{GL}$  (current versus local gate) characteristics for a suspended small bandgap SWNT device (with the back gate grounded) recorded from room temperature to 1.5 K (curve with drastic oscillations) using  $V_{sd} = 1$  mV bias. Inset: Hysteresis-free double-sweep data for  $I_{sd}$  versus  $V_{GL}$  recorded at room temperature. The two arrows correspond to back-and-forth gate sweeps. The  $I_{sd}$  versus  $V_{GL}$  curves recorded under the two sweep-directions overlap with each other; b) a 2D plot of conductance  $dI_{sd}/dV_{sd}$  versus  $V_{GB}$  and bias  $V_{sd}$  ( $V_{GL}$  fixed at  $-3.0$  V) for the p-channel of the SWNT. The color scale bar for the conductance at the right of the graph is in units of  $e^2/h$ ; c) a close up of (a) in a smaller gate range ( $V_{GL}$ ) of 2–5 V (bias = 1 mV) for the n-channel of the SWNT. Inset: A 2D plot of  $dI_{sd}/dV_{sd}$  versus  $V_{GB}$  and  $V_{sd}$  ( $V_{GL}$  set at 3.5 V). The two lines were drawn to highlight discrete electronic states due to quantum confinement along the tube length. Dark to bright colors correspond to conductance in the range of 0 to  $0.2 e^2/h$ .

ly disappears soon after (in a few seconds) the devices are placed in Ar, dry air, or vacuum (Figure 2 a inset). This differs from nanotubes resting on SiO<sub>2</sub> substrates and is attrib-

uted to the lack of water molecules adsorbed on nanotubes in a dry environment, and that suspended nanotubes are free from intimate contact with water molecules adsorbed on an SiO<sub>2</sub> substrate.<sup>[8]</sup>

The second interesting property of the suspended nanotube devices is that they appear to be “cleaner” quantum systems than nanotubes on substrates. At low temperatures, the devices (length of suspension ( $L$ ) investigated here  $\approx 400\text{--}700$  nm) exhibited characteristics corresponding to single quantum dots or interference resonators, without the complex dots-in-series behavior often observed for tubes on substrates. A representative small-bandgap semiconducting (SGS) SWNT<sup>[9]</sup> device is shown in Figure 2. The temperature dependence of the dip in the  $I_{sd}$  versus  $V_{GL}$  plot in Figure 2a shows activated transport. A small bandgap of  $E_g \approx 70$  meV is obtained by fitting the conductance ( $G$ ) at the dip to  $\exp(-E_g/2K_B T)$ . Transport through the p- and n-channels of the SWNT appear asymmetric, with higher conductance for the p-channel. At  $T=100$  K, the subthreshold swings are  $S \approx 150$  mV/decade and 1.2 V/decade for the p- and n-subthreshold regions, respectively (Figure 2a). At this temperature, the expected value for  $S^{[10]}$  is  $[(kT/e)\ln 10]/\alpha_{GL} \approx 130$  mV/decade if the Schottky barrier (SB) height is  $\approx 0$ , where  $\alpha_{GL} \approx 0.14$  is the local-gate efficiency factor (that is, the shift in Fermi level for a change in the gate voltage of  $\Delta V_{GL} = 1$  V) as deduced later. Comparison of the subthreshold swings of the p- and n-channels to the theory-predicted value suggests near zero and appreciable positive SBs<sup>[7,11]</sup> to the valence and conduction bands, respectively, between the SGS tube and the S and D electrodes. This is also consistent with a higher p-channel conductance than for the n-channel.

A lock-in technique (503 Hz, 50  $\mu\text{V}$  S/D bias) was used to perform  $dI_{sd}/dV_{sd}$  measurements for the p-channel of our suspended SWNT devices. When the local gate was set at a constant of  $V_{GL} = -3.0$  V,  $dI_{sd}/dV_{sd}$  versus  $V_{GB}$  and  $V_{sd}$  exhibits an interference pattern with conductance peaks ( $\approx 45$   $\mu\text{S}$ ,  $1.4e^2/h$ ) and valleys ( $\approx 15$   $\mu\text{S}$ ,  $0.5e^2/h$ ; Figure 2b). The conductance peaks at  $V_{sd} \approx 2.8$  mV corresponds to the length of the nanotube  $L \approx 620$  nm very well through  $V_c = hv_F/2L \approx 1.67$  meV/L ( $\mu\text{m}$ ), which suggests that the p-channel of the SGS tube behaves as a well-defined Fabry–Perot interference wave guide or resonator.<sup>[12–14]</sup>

The n-channel of the device exhibits clear Coulomb blockade (CB) behavior (Figure 2c), as probed by fixing  $V_{GL} = 3.5$  V and sweeping  $V_{GB}$ . The positive SBs to the conduction band gives rise to two contact barriers that confine the nanotube quantum dot (QD). Clean periodic CB features corresponding to a single QD were observed with a charging energy of  $E_c \approx 13$  meV. Since the length of the nanotube is 620 nm, a charging energy of  $\approx 13$  meV is higher than  $E_c \approx 5$  meV/L ( $\mu\text{m}$ ), that is, approximately 8 meV, which would be typical for nanotube QDs on SiO<sub>2</sub> substrates.<sup>[15]</sup> This variation is due to the low dielectric constant of the medium (air/vacuum) surrounding the suspended nanotube (compared to SiO<sub>2</sub> for tubes on a substrate), which gives rise to a lower total capacitance and thus a higher charging energy for the suspended nanotube. We find that  $E_c \approx 8$  meV/L ( $\mu\text{m}$ ) describes the charging energies of

suspended SWNTs well. The local-gate efficiency is estimated to be  $\alpha_{GL} = E_c/\Delta V_{GL} = 0.15$  where  $\Delta V_{GL} \approx 87$  mV is the period of Coulomb oscillation in Figure 2c. We also observed extra lines outside the CB diamonds (Figure 2c, inset), which correspond to discrete excited quantum confined states along the length of the tube. The energy scale of the lines is  $\approx 2$  meV, which matches the discrete level spacing<sup>[15]</sup> of  $\Delta E \approx 1$  meV/L ( $\mu\text{m}$ ) in the nanotube.

We note that clean and homogeneous quantum interferometers and QDs are reliably observed with large numbers of our suspended SWNT devices, and at much higher frequency than tubes on substrates with similar lengths between the S and D electrodes. This suggests that few defects exist in our SWNTs at the submicrometer length scale and that the lack of substrate–nanotube interactions can prevent the break up of nanotubes into segments due to local chemical effects or mechanical strains.

A third interesting feature of our suspended nanotube devices is the two-gate configuration. We have measured the conductance of the sample versus both gates, as shown in Figure 3. Conductance features (for example, peaks and

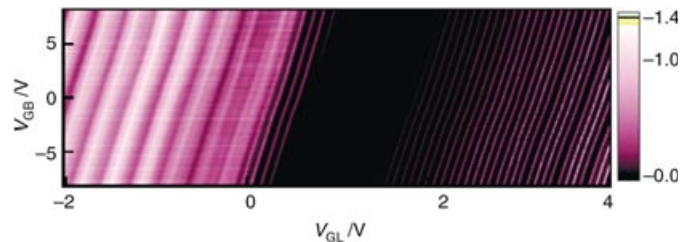


**Figure 3.** A 2D plot of conductance  $G$  versus  $V_{GL}$  and  $V_{GB}$  with  $V_{sd} = 1$  mV. The bright color corresponds to high conductance of  $1.4e^2/h$  and dark corresponds to zero conductance.

valleys) appear as parallel lines in the 2D plot, which indicates that the two gates are independent and additive. The slopes of the bright lines in  $G$  versus  $V_{GL}$  and  $V_{GB}$  can be used to deduce the ratio between the efficiencies of the two gates ( $\alpha_{GL}/\alpha_{GB} \approx 30$ ). This means that the local gate is  $\approx 30$  times more efficient than the back gate, or the local-gate capacitance  $C_{GL} \approx 30C_{GB}$ . The low efficiency of the back gate can be understood due to screening by the local gate (Figure 1). Note that the local-gate capacitance can be predicted by<sup>[16]</sup>  $C_{GL} \approx 2\pi\epsilon\epsilon_0 L/\ln(2h/r) \approx 5 \times 10^{-18}$  F, where  $\epsilon = 1$ , the nanotube radius  $r \approx 1$  nm, and the distance between the local gate and the nanotube (depth of trench)  $h = 300$  nm. This suggests that  $C_{GB} \approx C_{GL}/30 \approx 1.7 \times 10^{-19}$  F, which is in reasonable agreement with  $C_{GB} \approx 0.9 \times 10^{-19}$  F as measured from the CB data in the inset of Figure 2c. A potentially powerful aspect of the two-gate configuration is that under appropriate conditions, the local-gate electrostatic coupling could become sufficiently strong to induce appreciable mechanical strain in the nanotube. The less-effective global back gate could then be used as a sweeping gate to characterize the electromechanical effects to the suspended nanotube quantum dot. We are currently pursuing this interesting possibility, especially for electromechanical measurements at low temperatures.

The fourth interesting result obtained with our suspended SWNT devices is concerned with the high-bias transport properties of nanotubes when they are not resting on underlying substrates. This can shed light into the properties of nanotubes in their intrinsic state without significant roles played by the environment. For all of the suspended nanotubes that we have measured ( $L \approx 400\text{--}700\text{ nm}$ , resistance  $\approx 40\text{--}60\text{ k}\Omega$ ), we have consistently observed current saturation at the  $I_{\text{sat}} \approx 8\text{ }\mu\text{A}$  level, which is significantly lower than the saturation currents for nanotubes with a similar resistance that lie on substrates ( $15\text{--}20\text{ }\mu\text{A}$ ). Since current saturation at high fields in SWNTs is caused by the scattering of energetic ( $\approx 0.2\text{ eV}$ ) optical or zone-boundary phonons,<sup>[17–19]</sup> the lower saturation current in a suspended nanotube can be understood by the lack of a proximal thermally conductive  $\text{SiO}_2$  substrate for “heat sinking”. Electrical heating is rapid in suspended nanotubes and the heat cannot be efficiently conducted away to the surroundings. This leads to increased acoustic phonon scattering, which is responsible for the observed current decrease under increasing bias (seen as a slight negative differential conductance feature in Figure 4).

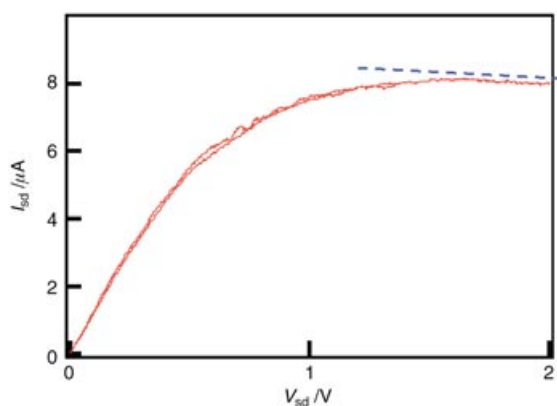


**Figure 4.**  $I_{\text{sd}}$  versus  $V_{\text{sd}}$  curve recorded for a suspended SWNT up to a high bias of  $V_{\text{sd}} = 2\text{ V}$ . The dashed line was drawn to highlight the slight negative differential conductance behavior.

In summary, a reliable method has been developed to obtain suspended SWNT devices with relatively good electrical contacts. Compared to nanotubes lying on substrates, the suspended devices exhibit little hysteresis behavior and manifest as well-defined single quantum dots or resonators.

The high-field saturation current caused by optical phonon scattering in suspended nanotubes is low. The multiple-gate design may facilitate future investigation of the electromechanical properties of nanotubes.

### Acknowledgement

This work was supported by MARCO MSD, a NSF-NIRT grant, SRC/AMD, DARPA/MTO, a Packard Fellowship, Sloan Research Fellowship and a Camille Dreyfus Teacher–Scholar Award.

- [1] T. W. Tomblor, C. W. Zhou, L. Alexseyev, J. Kong, H. J. Dai, L. Lei, C. S. Jayanthi, M. J. Tang, S. Y. Wu, *Nature* **2000**, *405*, 769.
- [2] D. A. Walters, L. M. Ericson, M. J. Casavant, J. Liu, D. T. Colbert, K. A. Smith, R. E. Smalley, *Appl. Phys. Lett.* **1999**, *74*, 3803.
- [3] J. Nygard, D. H. Cobden, *Appl. Phys. Lett.* **2001**, *79*, 4216.
- [4] N. R. Franklin, Q. Wang, T. W. Tomblor, A. Javey, M. Shim, H. J. Dai, *Appl. Phys. Lett.* **2002**, *81*, 913.
- [5] J. Cao, Q. Wang, H. J. Dai, *Phys. Rev. Lett.* **2003**, *90*, 157 601.
- [6] E. D. Minot, Y. Yaish, V. Sazonova, J. Y. Park, M. Brink, P. L. McEuen, *Phys. Rev. Lett.* **2003**, *90*, 156401.
- [7] A. Javey, J. Guo, Q. Wang, M. Lundstrom, H. J. Dai, *Nature* **2003**, *424*, 654.
- [8] W. Kim, A. Javey, O. Vermesh, Q. Wang, Y. M. Li, H. J. Dai, *Nano Lett.* **2003**, *3*, 193.
- [9] C. W. Zhou, J. Kong, H. J. Dai, *Phys. Rev. Lett.* **2000**, *84*, 5604.
- [10] S. M. Sze, *Physics of semiconductor devices*, Wiley, New York, **1981**.
- [11] S. Heinze, J. Tersoff, R. Martel, V. Derycke, J. Appenzeller, P. Avouris, *Phys. Rev. Lett.* **2002**, *89*, 6801.
- [12] W. Liang, M. Bockrath, D. Bozovic, J. Hafner, M. Tinkham, H. Park, *Nature* **2001**, *411*, 665.
- [13] J. Kong, E. Yenilmez, T. W. Tomblor, W. Kim, L. Liu, C. S. Jayanthi, S. Y. Wu, R. B. Laughlin, H. J. Dai, *Phys. Rev. Lett.* **2001**, *87*, 106801.
- [14] D. Mann, A. Javey, J. Kong, Q. Wang, H. J. Dai, *Nano Lett.* **2003**, *3*, 1541.
- [15] J. Nygard, D. H. Cobden, M. Bockrath, P. L. McEuen, P. E. Lindelof, *Appl. Phys. A* **1999**, *69*, 297.
- [16] S. Ramo, J. R. Whinnery, T. V. Duzer, *Fields and Waves in Communication Electronics*, Wiley, New York, **1994**.
- [17] Z. Yao, C. L. Kane, C. Dekker, *Phys. Rev. Lett.* **2000**, *84*, 2941.
- [18] A. Javey, J. Guo, M. Paulsson, Q. Wang, D. Mann, M. Lundstrom, H. J. Dai, *Phys. Rev. Lett.* **2004**, *92*, 106804.
- [19] J. Y. Park, S. Rosenblatt, Y. Yaish, V. Sazonova, H. Ustunel, S. Braig, T. A. Arias, P. W. Brouwer, P. L. McEuen, *Nano Lett.* **2004**, *4*, 517.

Received: June 15, 2004

Published online on September 16, 2004